Driving Performance Analysis of the Adaptive Cruise Controlled Vehicle with a Virtual Reality Simulation System

Seong-Jin Kwon, Jee-Hoon Chun, Suk Jang, Myung-Won Suh*
School of Mechanical Engineering, Sungkyunkwan University,
300 Chunchun-dong, Jangan-gu, Suwon 440-746, Korea

Nowadays, with the advancement of computers, computer simulation linked with VR (Virtual Reality) technology has become a useful method for designing the automotive driving system. In this paper, the VR simulation system was developed to investigate the driving performances of the ASV (Advanced Safety Vehicle) equipped with an ACC (Adaptive Cruise Control) system. For this purpose, VR environment which generates visual and sound information of the vehicle, road, facilities, and terrain was organized for the realistic driving situation. Mathematical models of vehicle dynamic analysis, which includes the ACC algorithm, have been constructed for computer simulation. The ACC algorithm modulates the throttle and the brake functions of vehicles to regulate their speeds so that the vehicles can keep proper spacing. Also, the real-time simulation algorithm synchronizes vehicle dynamics simulation with VR rendering. With the developed VR simulation system, several scenarios are applied to evaluate the adaptive cruise controlled vehicle for various driving situations.

Key Words : Intelligent Transport Systems, Advanced Safety Vehicle, Adaptive Cruise Control, Virtual Reality, Vehicle Dynamics, Simulation

1. Introduction

The rapid increase of automobiles has caused worldwide problems such as safety against traffic accidents, traffic congestion, environmental pollution, and economical inefficiency. ITS (Intelligent Transport Systems) is an effort to resolve these problems with information, communication, and control strategy. It is believed to be the next generation technology for an automobile industry and transportation organizations (Hayashi, 1998 ; Kubozuka, 2002). The research and development supporting this effort has progressed actively in the belief that ITS will improve transport network flow, enhance driver safety, reduce environmental impact, and provide large commercial market opportunities (Shladover et al., 1991 ; Lee, 2003).

ASV (Advanced Safety Vehicle) for ITS can be applied to intelligent and automated vehicles. ASV includes diverse systems, e.g., ACC (Adaptive Cruise Control), FVCWS (Forward Vehicle Collision Warning System), LDWS (Lane Departure Warning System), FCAAS (Forward Collision Avoidance Assistance System), LCDAS (Lane Change Decision Aid System), and so on. Above all, the ACC system can control the throttle and the brake functions by recognizing the road environment to maintain traffic safety (Tamura and Furukawa, 1998).

The ACC system has been extensively researched and some of ACC systems have been realized. Wang and Rajaman (2002) proposed a design of the ACC system that can improve traffic flow and ensure safe vehicle operation on the motorway. The spacing policy, referred to as a variable time-gap policy, led to stable traffic flow and a higher road capacity. Holve et al.(1996)

* Corresponding Author,
E-mail : suhmw@yurim.skku.ac.kr
TEL : +82-31-290-7447; **FAX** : +82-31-290-7447
School of Mechanical Engineering, Sungkyunkwan University, 300 Chunchun-dong, Jangan-gu, Suwon 440-746, Korea. (Manuscript **Received** February 4, 2005; **Revised** August 10, 2005)

described the procedure of fuzzy rule generation, which was used in the development of an adaptive fuzzy controller for vehicle speed and distance control. Seto et al.(1998) developed a headway distance control system using inter-vehicle communication to control vehicle longitudinal motion. Lee and Chang (2000) proposed additional schemes, which are a gear shift-down controller and a predictive correction method, to enhance the sliding mode controller's performance for autonomous cruise control. Also, Lee et al.(2001) proposed a throttle/brake control law for the ACC systems.

The previous researches focused on the design and performance of the longitudinal controller for the ACC system. In these researches, the experiment and computer simulation analyzed the dynamic characteristics of the proposed longitudinal controller. However, the experiment required enormous time and cost, and it was sometimes dangerous to evaluate the vehicle in an extreme situation, while computer simulation evaluated the vehicle only for pre-fixed scenarios, for which driver behavior characteristics were not considered. A method to supplement the two methods, computer simulation linked with VR (Virtual Reality) technology is used. It enables MILS (Man-In-the Loop Simulation) in the realistic driving situation by using feedbacks of the 3D images and sound effects, which are correlated with vehicle's motion. Also, the VR simulation method can overcome the practical limitations of time, cost, and inconvenient outfitting of test vehicles and conducting test-track experiments (Redmill et al., 2000).

In this study, the VR simulation system is developed to analyze the dynamic characteristics of the ACC system. For this purpose, the VR system, which generates visual and sound information in virtual space, is organized for the realistic driving situation. The ACC simulation system, which contains the mathematical vehicle dynamics models and the ACC algorithm, is constructed for computer simulation. Also, the real-time simulation algorithm synchronizes the VR system with the ACC simulation system. With the developed VR simulation system, the proposed ACC algorithm is verified by the experiment, and various scenarios are applied to the adaptive cruise controlled vehicle to evaluate its dynamic characteristics.

2. System Configuration

This chapter explains the configuration of the VR simulation system developed in this paper. The VR simulation system consists of the VR system and the ACC simulation system. The VR system embodies visual and sound information. The ACC simulation system performs the vehicle dynamics analysis of the ACC vehicle. Microsoft Visual C++ 6.0 programming language was utilized to develop this system.

2.1 Hardware configuration

The configuration of the VR simulation system is shown in Fig. 1. The graphic system represents visual information, the audio system gives sound information, and the driver system receives driver operation information while the computer parts regulate the entire system. The hardware of the VR simulation system was reconstructed from the SVPG (Sungkyunkwan Univ. Virtual Proving Ground) by Suh et al.(2002) for this study.

2.2 Software configuration

The components of the VR simulation system are shown in Fig. 2. The VR system expresses the realistic driving situation of VR database through

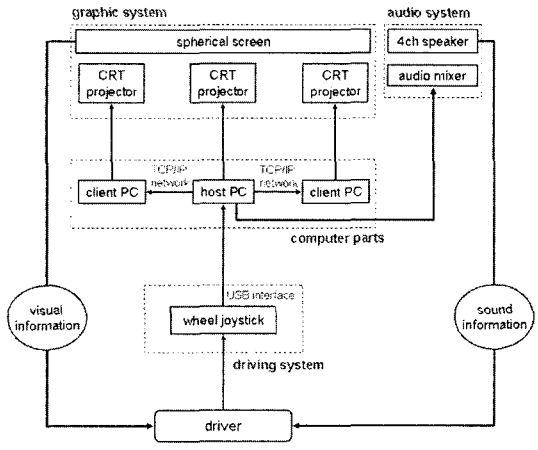

Fig. 1 Configuration of the VR simulation system

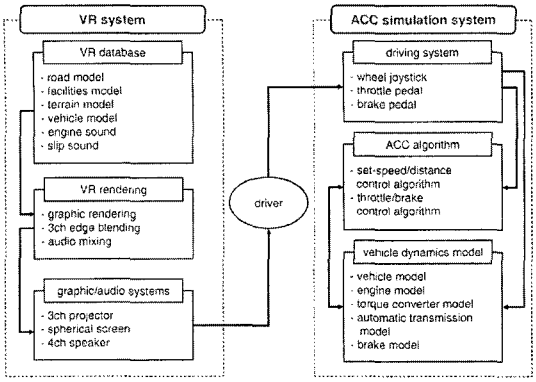

Fig. 2 Components of the VR simulation system

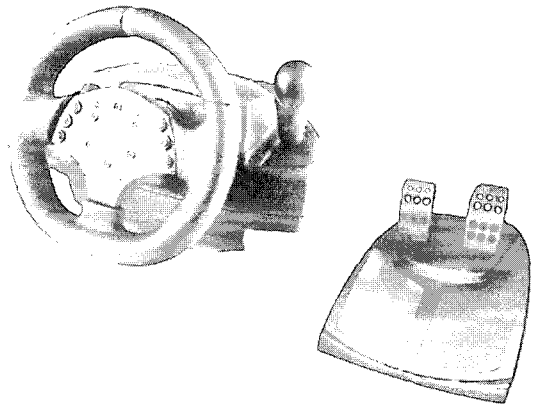

Fig. 3 Wheel joystick

the graphic and audio systems. Visual information of VR database includes the road, facilities, terrain, and vehicle. Sound information of VR database is constructed by digital sampling of the real vehicle's engine and slip sound. The ACC simulation system analyzes the dynamic characteristics with the mathematical vehicle dynamics model and the ACC algorithm. Also, the real-time connection between the VR system and the ACC simulation system will be discussed in the next section of the system integration.

3. ACC Simulation System

This chapter explains the driving system, vehicle dynamics model, and the ACC algorithm used in this paper. The driver system receives driver operation information, and the vehicle dynamics model, which has the 8 degrees-of-freedom including nonlinear subcomponents, calculates the vehicle motion. This vehicle dynamics model is refined by comparisons with vehicle test information. The ACC algorithm is proposed to control the throttle and the brake of vehicles automatically instead of a human driver.

3.1 Driving system

To simplify the data processing of the vehicle's operation, the wheel joystick is used instead of the chassis and sensors of the real vehicle. The joystick is the Momo racing wheel made by Logitech, and it is composed of a steering wheel and two pedals as described in Fig. 3. Although this driving system has simplified the real vehicle, this system with VR environment could provide the reasonable simulation results (Jang et al., 2005).

Table 1 Joystick data mapping

	Joystick input value	Mapping value
steering wheel angle	−12400~12400	−120~120 degree
throttle ratio	0~221400	0~100%
brake pressure	0~−221400	0~70 bar

To make the interface software between the wheel joystick and the host PC, the DirectX SDK (Software Development Kit) and CDX (Class for the DirectX) are utilized. The interface cable is USB (Universal Serial Bus) 2.0, and the input data of the wheel joystick are reflected in the vehicle dynamics model, as described in Table 1.

3.2 Vehicle dymamics model

In this paper, the vehicle dynamics model is comprised of the 8 degrees-of-freedom vehicle model developed by Kim et al.(1999) and the subcomponent models developed by Suh et al. (1999). It is constructed to analyze the dynamic characteristics according to driver's operation conditions such as the throttle ratio and brake pressure, and steering wheel angle. In the vehicle dynamics model, the tractive force is calculated with the power train model composed of the engine, torque converter, automatic transmission, drive shaft, and wheels according to the throttle

Table 2 Vehicle parameter

Parameter	Unit	Value
vehicle mass	kg	1900
wheelbase	m	2.965
tire rolling radius	m	0.406
1st gear ratio	—	3.590
2nd gear ratio	—	2.190
3rd gear ratio	—	1.410
4th gear ratio	—	1.000
5th gear ratio	—	0.830
final reduction gear ratio	—	2.820

ratio. The braking force is calculated by the brake model based on the brake pressure. The cornering force is calculated by the change of the front tire angle according to the steering wheel angle. The vehicle parameters of the ACC vehicle are used for vehicle dynamics simulation as detailed in Table 2.

The vehicle tests were carried out to verify the proposed vehicle dynamics model. The rolling resistance coefficient and the aerodynamic drag coefficient were estimated by the coastdown test with the initial vehicle velocity of 130 km/h. As the result of the coastdown test, the rolling resistance coefficient and the aerodynamic drag coefficient were calculated to be 0.0244 and 0.374, respectively, by the TRIAS test method (Korean Society of Automotive Engineers, 1996). To check the validity of these coefficients, the coastdown test was compared with the vehicle dynamics simulation as shown in Fig. 4(a).

The accelerating test was implemented for various ranges of vehicle velocity while the operation ratios of the throttle pedal were regulated to 30%, 60%, and 100%. Using the velocity data acquired from the vehicle test, the vehicle dynamics model was verified. At the operation ratio of the throttle pedal of 60% and the velocity range of 0 km/h to 130 km/h, the accelerating test was compared with the vehicle dynamics simulation as shown in Fig. 4(b). Also, when the operation ratio of the throttle pedal was 100%, the acceleration time from 0 km/h to 100 km/h was 10.971 s in simulation and 9.975 s in the vehicle test. The simulation result confirmed that the vehicle dynamics simulation can suitably describe the accelerating performance of a real vehicle.

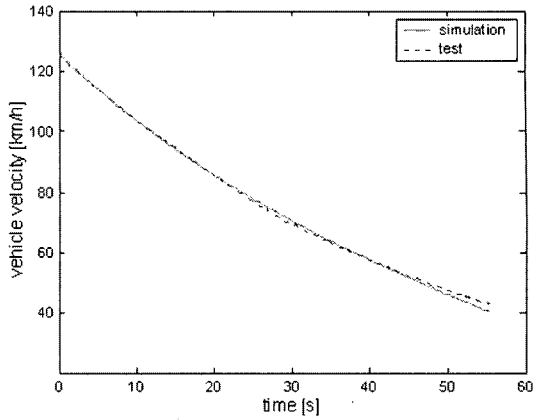

(a) Case of the coastdown test

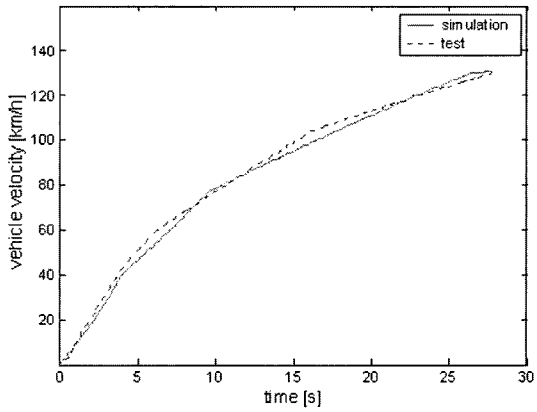

(b) Case of the accelerating test

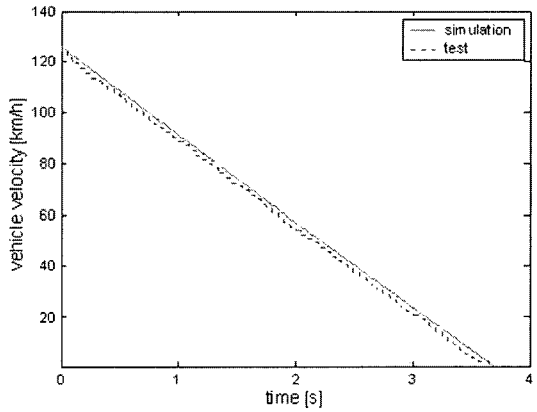

(c) Case of the braking test

Fig. 4 Verification of the vehicle dynamics model

The braking test was conducted by measuring the variation of the vehicle velocity, as the operation ratios of the brake pedal force were regulated to 30%, 60%, and 100%. The brake pressure was

assumed to have a linear relationship with the brake pedal force. The simulation and test were compared, as shown in Fig. 4(c), at the operation ratio of the brake pressure ratio of 100% and the initial vehicle velocity of 130 km/h.

3.3 ACC algorithm

The vehicle equipped with the ACC system includes the sensors to detect driving information, the control strategy to decide the desired vehicle response, and the actuators to perform the desired vehicle response. The ISO (International Organization for Standardization) 15622 (2002) represents the basic configuration of the ACC system, as shown in Fig. 5. The ACC algorithm is operated with the driver, vehicle, and environment information.

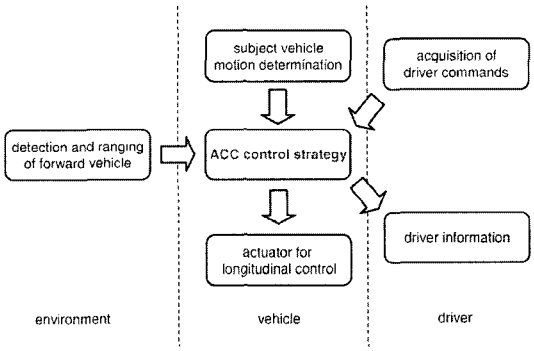

Fig. 5 Functional ACC elements

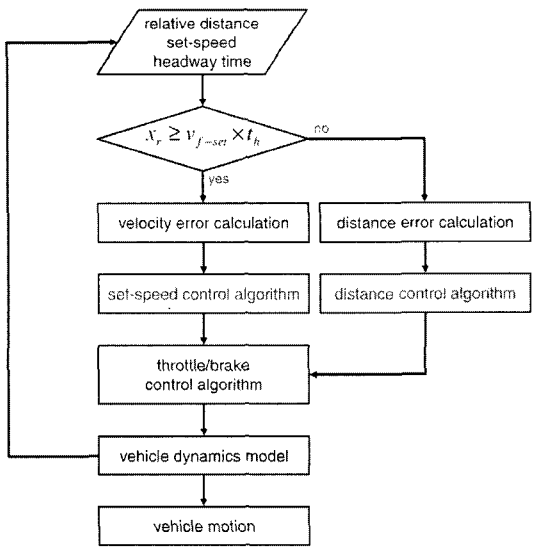

Fig. 6 Flow chart of the ACC algorithm

In this study, the ACC algorithm was developed as shown in Fig. 6. The proposed ACC algorithm has the unique switching logic which determines either the distance control algorithm or the set-speed control algorithm. In addition, the proposed ACC algorithm contains the system requirements which are suggested by ISO 15622 (2002). Those are the basic control strategy, functionality, basic driver interface and intervention capabilities and operational limits.

First, the subject vehicle (SV) equipped with the ACC system recognizes the driving situation including the leading vehicle (LV). The subject vehicle selects the control algorithm, either the set-speed control algorithm or the distance control algorithm. In the set-speed control algorithm, the desired acceleration is calculated from the set-speed and the velocity of the subject vehicle. In the distance control algorithm, the desired acceleration is derived from the velocity of the subject vehicle, the headway time, and the relative distance between the subject vehicle and the leading vehicle. Based on the desired acceleration, the throttle ratio and the brake pressure to the vehicle dynamics model are calculated by the throttle/brake control algorithm.

3.3.1 Set-speed/distance control algorithm

The ACC algorithm is divided into the set-speed control algorithm and the distance control algorithm. The proper control algorithm can be selected by using the following equation.

$$x_r \geq v_{f-set} \times t_h \tag{1}$$

where v_{f-set} is the set-speed of the subject vehicle, x_r is the relative distance between the subject vehicle and the leading vehicle, and t_h is the headway time. The left side of the Eq. (1) means the relative distance measured from the sensor, and the right side means the desired set-distance. Therefore, when Eq. (1) is satisfied or the subject vehicle cannot recognize the leading vehicle, the set-speed control algorithm is implemented; otherwise, the distance control algorithm is implemented.

The set-speed control algorithm is shown in Fig. 7(a). The error (e_1) between the set-speed and the velocity of the subject vehicle (v_f) is shown as follows:

$$e_1 = v_{f-set} - v_f \tag{2}$$

The distance control algorithm includes both the headway time policy and the fixed distance policy. In this study, the headway time policy is used as shown in Fig. 7(b). The desired distance is calculated by using the velocity of the subject vehicle and the headway time as follows:

$$x_{r-des} = v_f \times t_h \tag{3}$$

The error (e_2) between the desired distance and the relative distance is obtained:

$$e_2 = x_r - x_{r-des} \tag{4}$$

In this study, to calculate the desired acceleration (a_{f-des}) of the subject vehicle according to the errors described in the Eqs. (2) and (4), the sliding controller researched by Fujioka et al. (1995) is adopted. Also, as mentioned in the ISO 15622, the sensor cannot measure the relative distance exactly when the subject vehicle approaches the leading vehicle very closely. For this case, we suggest an additional algorithm in which the subject vehicle is decelerated unconditionally to increase the relative distance. In this paper, the minimum detection range of the sensor is assumed to 4 m.

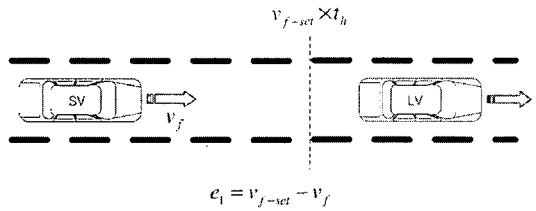

(a) Set-speed control algorithm

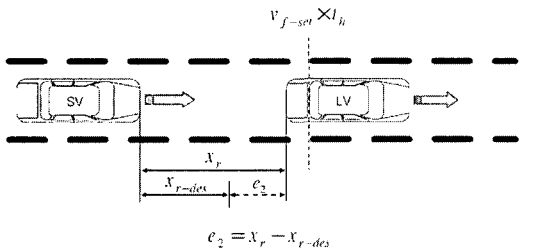

(b) Distance control algorithm

Fig. 7 Overview of the set-speed/distance control algorithm

3.3.2 Throttle/brake control algorithm

The throttle/brake control algorithm was constructed to calculate the vehicle motion based on the desired acceleration calculated from the set-speed/distance control algorithm. The main objective of the throttle/brake control algorithm is to control the throttle and the brake of vehicles automatically instead of a human driver, as shown in Fig. 8.

Based on the desired acceleration, the desired tractive force, and the desired engine torque (T_{e-des}) are calculated successively (Kwon et al., 2004). The desired engine torque is as follows:

$$T_{e-des} = \frac{R(Ma_{f-des} + F_D)}{N_t N_f} \tag{5}$$

where R is the rolling radius, M is the vehicle mass, F_D is the road load, N_t is the automatic transmission gear ratio, and N_f is final reduction gear ratio. Finally, the desired throttle ratio (α) can be obtained by means of the inverse engine map according to the desired engine torque and the engine speed.

$$\alpha = f_e^{-1}(T_{e-des}, \omega_e) \tag{6}$$

where f_e^{-1} is the function of the inverse engine map and ω_e is the angular speed of the engine. When the desired throttle ratio is positive, the throttle actuator is operated and the tractive force is calculated with the power train model in the vehicle dynamics model. In addition, when the

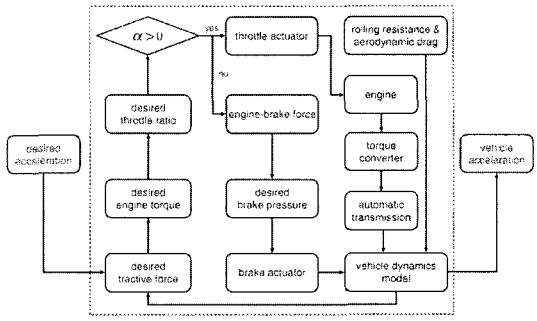

Fig. 8 Flow chart of the throttle/brake control algorithm

desired acceleration is negative, the desired brake pressure ($P_{b\text{-}des}$) can be obtained :

$$P_{b\text{-}des}=\frac{1}{K_b}\{-R(Ma_{f\text{-}des}+F_D)\} \qquad (7)$$

where K_b is the brake gain. From the desired brake pressure, the braking force is calculated by the brake model in the vehicle dynamics model. The output variable of the throttle/brake control algorithm, which represents the actual vehicle acceleration, calculates the vehicle motion.

4. VR System

The VR system consists of VR database, VR rendering, and graphic/audio systems. The VR system provides a driver with natural interaction, sufficient immersion, and realistic VR database. The structure and construction of VR database influences the rendering performance closely. Therefore, the modeling and rendering methods for VR database are investigated in this chapter.

4.1 VR database

The VR database consists of the vehicle, road, facilities, and terrain. The road and the terrain describe the real proving ground and the facilities include tollgate, guardrail, traffic sign, and so on. Also the vehicle includes the 3D models of the ACC vehicle and the conventional vehicles. Multigen Creator ver.2.5.1 (1999) is utilised as a 3D modeling tool. To ensure the real-time rendering performance, we use the polygon reduction method and various texture mapping methods such as the alpha blending texture mapping that gives transparency ; the texture MIP-mapping (Multum in Parvo), which simplifies the texture rendering ; and the billboard, which is the 2D modeling method based on the texture.

4.2 VR rendeing

The rendering methods such as the weather, illumination, and camera viewpoint are applied to the 3D objects. Also, the hidden surface removal, shading, culling, and LOD (Level of Detail) are used to improve the rendering performance.

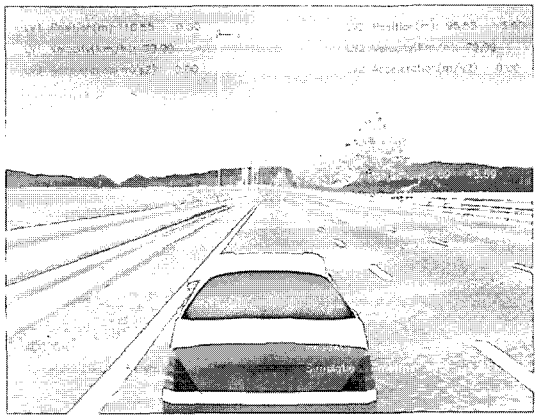

(a) Viewpoint at the subject vehicle

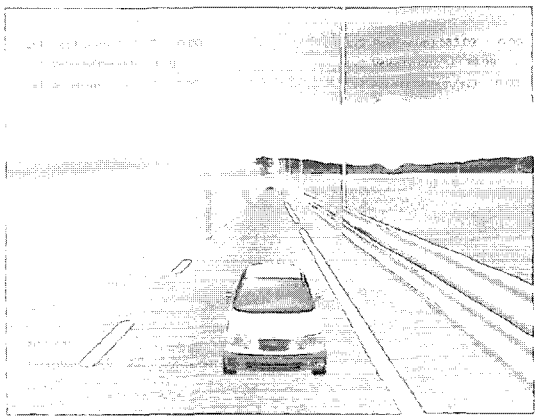

(b) Viewpoint at the leading vehicle

Fig. 9 VR rendering images

In this study, the real-time rendering tool is Vega 3.7 MP (1999) based on Open GL. In addition, we added functions such as supporting multi-viewpoint, indicating of driving information, and expressing of the sensor scope for driver's convenience. Figure 9 shows the VR rendering images of the VR database.

4.3 Graphic system

In this paper, the spherical screen and three-channel CRT (Cathode Ray Tube) projectors are adopted to supply the driver with realistic immersion as shown in Fig. 10. This system has 150° horizontal field of view that is wider than the 130° of a human's general view. The graphic server for the projection system consists of 3 PCs, which are connected by TCP/IP (Transmission Control Protocol/Internet Protocol) network for

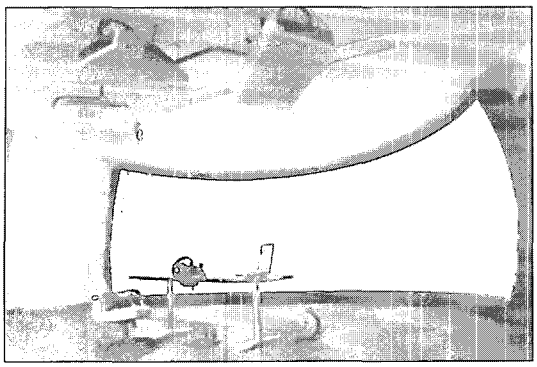

Fig. 10 Three-channel projection system

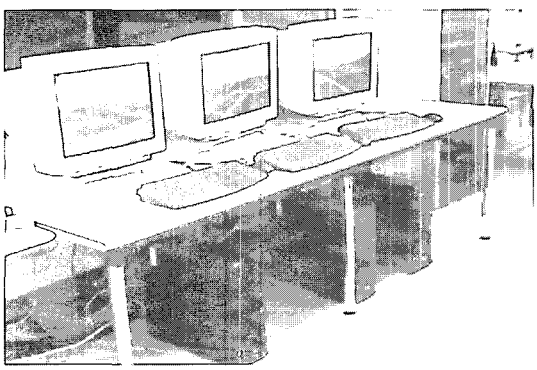

Fig. 11 Host PC and client PCs

distributed processing to reduce the rendering load as shown in Fig. 11. The visual images on the screen are synchronized by edge blending at the boundaries of each channel.

4.4 Audio system

The audio system consists of the host PC which generates sound information, the audio mixer which amplifies sound information, and 4 channel speakers which supply sound effects to the driver. Audio data are obtained by digital sampling of real engine sound and slip sound of a wheel. To create a realistic driving situation, sound information is supplied to the driver in real-time according to the response of the vehicle dynamics model.

5. System Integration

The connection between the VR system and the ACC simulation system strongly influences the real-time performance of the ACC VR simulation system. Also, the coordinate systems of these systems are mathematically synchronized to reflect the real world.

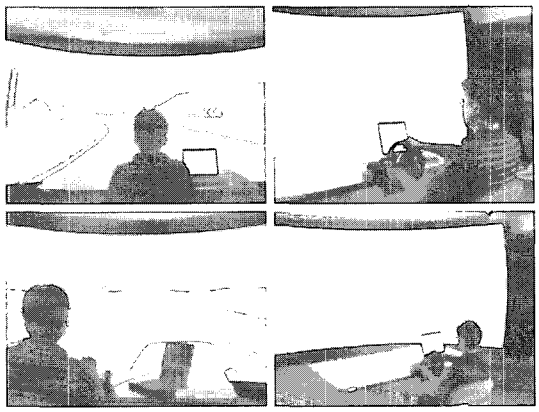

Fig. 12 ACC test driving using the developed VR simulation system

5.1 Connection between VR system and ACC simulation system

The vehicle position and motion in the VR system is determined by the simulation result of the ACC simulation system. However, the vehicle dynamics model is operated in the coordinate system of the real world ; and the VR system is operated in the coordinate system of the VR world. Therefore, the coordinate systems are mathematically synchronized.

5.2 Real-time VR simulation

The simulation time step of the vehicle dynamics model is fixed to 1ms for simulation reliability. We utilized the SDK's library function to ensure the real-time characteristics of ACC simulation. As the result, the rendering performance can maintain 40 fps (frames per second) during simulation. This frame rate is much higher than the general frame rate (16~24 fps) that a human being can recognize as continuous motion. The stable rendering performance perceived by the driver as the real driving situation is achieved in this study. Figure 12 shows the ACC test driving using the developed VR simulation system.

6. Application Examples

To verify the proposed ACC algorithm and to evaluate usefulness of the developed VR simulation system, simulations have been carried out in various conditions. One scenario was verified by comparing the simulation results with experimental results. Two scenarios were considered as application examples: first, a deceleration situation and second, a cut-in situation.

6.1 Verification through experiment

As shown in Fig. 13(a), in the deceleration situation, the leading vehicle in front of the subject vehicle maintains a constant velocity. After that, the leading vehicle reduces its velocity at a constant deceleration while the subject vehicle follows the leading vehicle with the distant control algorithm.

In the first case of this scenario, the initial velocities of the leading vehicle and the subject vehicle are 120 km/h, and then the leading vehicle changes its velocity from 120 km/h to 60 km/h at the deceleration rate of 1 g/3. In the second case, the initial velocities of the leading vehicle and the subject vehicle are 100 km/h, and then the leading vehicle changes its velocity from 100 km/h to 80 km/h at the deceleration rate of 1 g/3.

The average deceleration of the subject vehicle is shown in Table 3, which compares the simulation results with experiment results according to the headway time. The deceleration derived from ACC algorithm doesn't exceed $\pm 2\ m/s^2$ according to ISO 15622. As the errors between simulation and experiment are less than 6%, the proposed ACC algorithm is proved that it is similar with the real adaptive cruise controlled vehicle. Based on these results, the developed ACC algorithm can be used to evaluate the ACC vehicle and to analyze driving behavior in various conditions.

6.2 Deceleration situation

As shown in Fig. 13(a), in the deceleration

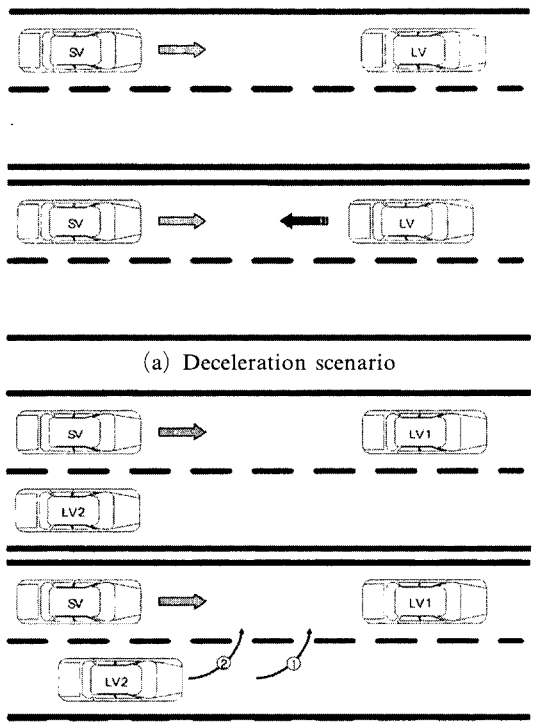

(a) Deceleration scenario

(b) Cut-in scenario

Fig. 13 Scenarios for the VR simulation system

Table 3 Comparison between simulation and experiment

Velocity variation of LV	Headway time	Average deceleration (Experiment)	Average deceleration (Simulation)	Error
120 → 60 km/h	1.0 s	1.961 m/s^2	1.998 m/s^2	1.9%
	1.2 s	1.930 m/s^2	1.952 m/s^2	1.1%
	1.4 s	2.000 m/s^2	1.998 m/s^2	0.01%
	1.5 s	1.961 m/s^2	1.998 m/s^2	1.9%
100 → 80 km/h	1.0 s	2.121 m/s^2	1.998 m/s^2	5.8%
	1.2 s	1.800 m/s^2	1.897 m/s^2	5.1%
	1.4 s	1.790 m/s^2	1.746 m/s^2	2.5%
	1.5 s	2.121 m/s^2	1.997 m/s^2	5.8%

situation, the leading vehicle in front of the subject vehicle maintains a constant velocity from 0 s to 12 s. After that, the leading vehicle reduces its velocity at a constant deceleration rate.

In the first case of this scenario, the initial velocity of the leading vehicle is 110 km/h, and the set-speed of the subject vehicle is 120 km/h. Also, the headway time is set to 1.0 s, and the constant deceleration rate of the leading vehicle is 0.1 g. As shown in Fig. 14 of the simulation results, while the leading vehicle maintains the constant velocity of 110 km/h, the subject vehicle initially accelerates to follow the set-speed control algorithm. As the relative distance between the subject vehicle and the leading vehicle is decreased, the subject vehicle detects the leading vehicle. The subject vehicle follows the distance control algorithm to maintain the desired relative distance. Then, the leading vehicle changes its velocity from 110 km/h to 80 km/h at the deceleration rate of 0.1 g. The subject vehicle properly controls the relative distance corresponding to the leading vehicle. The simulation results show that the proposed ACC algorithm is stable when the deceleration of the leading vehicle is relatively small.

The second case is an extreme situation. Its initial condition is the same to the first case. The constant deceleration rate of the leading vehicle is 0.5 g. As shown in Fig. 15 of the simulation results, in the beginning, the subject vehicle is accelerated from 110 km/h to 120 km/h to follow the set-speed control algorithm. Also, the subject vehicle changes its control strategy to properly follow the distance control algorithm. Then, the leading vehicle changes its velocity from 110 km/h to 60 km/h at the deceleration rate of 0.5 g. Although the subject vehicle detects the deceleration of the leading vehicle, the subject vehicle cannot follow the deceleration of the leading vehicle and collision occurs. In this study, the acceleration of the subject vehicle is limited not to exceed $\pm 2\ m/s^2$ as mentioned in ISO 15622.

To avoid the collision, we simulated case 2 with the change in the headway time from 1.0 s to 1.5 s. As shown in Fig. 16 of the simulation

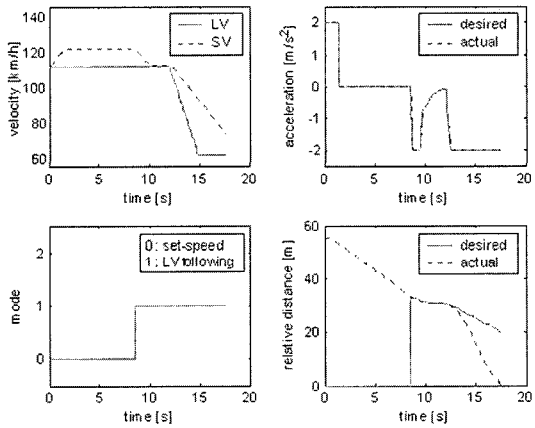

Fig. 15 Simulation result of 0.5 g deceleration scenario (t_h=1.0 s)

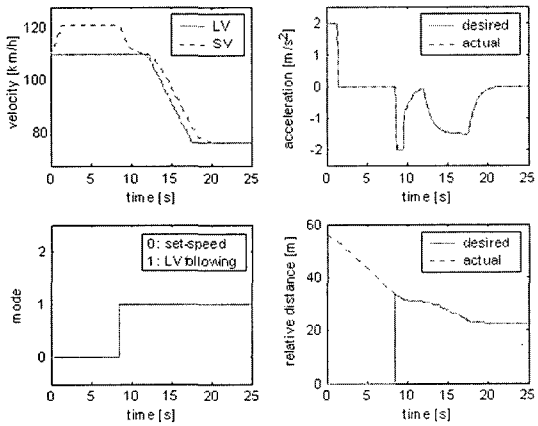

Fig. 14 Simulation result of 0.1 g deceleration scenario (t_h=1.0s)

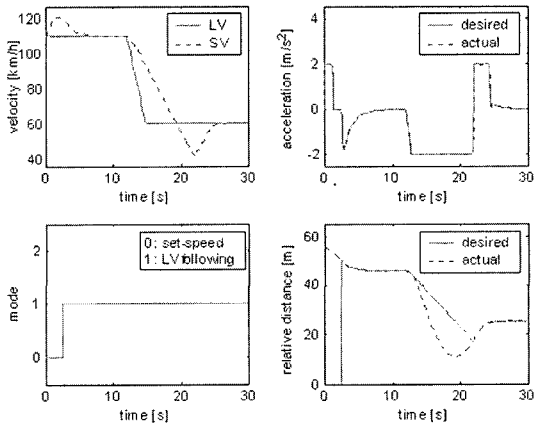

Fig. 16 Simulation result of 0.5 g deceleration scenario (t_h=1.5 s)

results, when the leading vehicle decelerates with 0.5 g, the subject vehicle cannot follow the desired relative distance accurately. However, the subject vehicle can avoid collision because the headway time affects the desired distance to be long.

6.3 Cut-in situation

As shown in Fig. 13(b), in the cut-in situation, the leading vehicle 1 in front of the subject vehicle maintains a constant velocity. After that, the leading vehicle 2 of the right lane changes lanes to cut in between the leading vehicle 1 and the subject vehicle. Then, the leading vehicle 2 decelerates with 0.1 g.

In the first case of this scenario, the initial velocities of the leading vehicle 1 and the leading vehicle 2 are 80 km/h, and the set-speed of the subject vehicle is 100 km/h. Moreover, the headway time is set to 1.0 s. The leading vehicle 2 cuts in with sufficient distance in front of the subject vehicle. As shown in Fig. 17 of the simulation results, in the beginning, the subject vehicle accelerates to follow the set-speed control algorithm because the leading vehicle 1 is far from the subject vehicle. After detection of the leading vehicle 1, the subject vehicle decelerates to follow the distance control algorithm to maintain the desired distance between the subject vehicle and the leading vehicle 1. When the leading vehicle 2 changes lanes 18 m in front of the subject vehicle, the vehicle that the subject vehicle follows is changed from the leading vehicle 1 to the leading vehicle 2. Also, the subject vehicle maintains the desired distance according to prescribed actions given by the distance control algorithm. The simulation results show that the subject vehicle can change the adequate control algorithm according to the various driving situations.

In the second case, although the initial condition is same to the first case, the leading vehicle 2 cuts in with insufficient distance in front of the subject vehicle. As shown in Fig. 18 of the simulation results, the leading vehicle 2 tries to change lanes 8 m in front of the subject vehicle. The subject vehicle also maintains the desired distance. Although the vehicle that the subject vehicle follows is changed from the leading vehicle 1 to the leading vehicle 2, the driver could be anxious about the collision because of the insufficient relative distance. Also, this case is a dangerous situation for a possible collision.

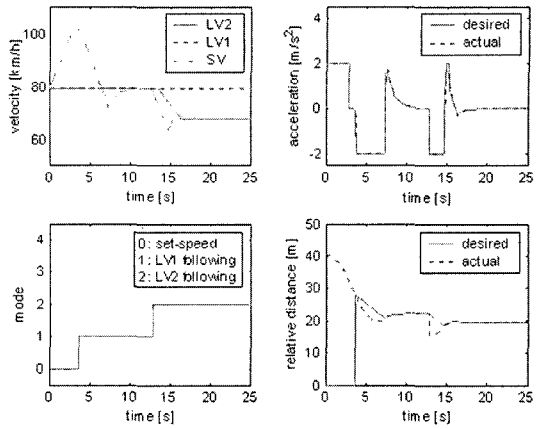

Fig. 17 Simulation result of the cut-in scenario (t_h= 1.0 s, minimum relative distance=18 m)

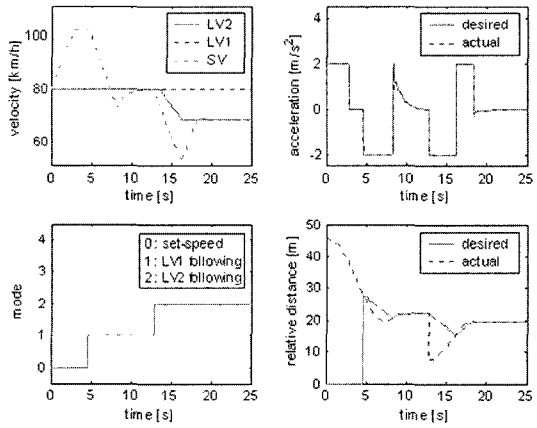

Fig. 18 Simulation result of the cut-in scenario (t_h=1.0 s, minimum relative distance=8 m)

7. Conclusion

In this paper, the VR simulation system was developed to analyze the driving characteristics of the ACC vehicle for the various driving situations. The VR system and the ACC simulation system were constructed separately. The VR system describes visual and sound information, and the ACC simulation system performs real-time

vehicle dynamics simulation of the ACC vehicle. Also, the VR system was synchronized with the ACC simulation system to integrate the systems.

To validate the developed system and the proposed ACC algorithm, several scenarios were applied to the VR simulation system. The proposed ACC algorithm is verified by the experiment. The VR simulation system also overcame the limitation of the experiment and computer simulation. The developed system can be used to evaluate the ACC vehicle and to analyze driving behavior. Consequently, we conclude the following.

(1) The ACC vehicle can change the specific control algorithms according to various driving situations. The ACC vehicle stably follows both the set-speed control algorithm and the distance control algorithm. However, the ACC vehicle can be crashed when the leading vehicle decelerates by 0.5 g or tries the cut-in with relative distance by 8 m.

(2) The desired distance of the ACC algorithm is determined by the headway time, which the driver sets up. The more the headway time, the more stable the ACC vehicle. On the other side, more headway time can invite frequent cut-in's by other vehicles and decrease the efficiency of transport network flow.

(3) In this study, the dynamic characteristics and driving performance of the ACC vehicle were analyzed. These results can be based on the derivation of the safety standards which corresponds the correlation with the driver, road, and vehicle.

Acknowledgments

This work was supported by grant No. R01-2004-000-10938-0 from the Basic Research Program of the Korea Science & Engineering Foundation. Also, this work was financially supported by the Ministry of Education and Human Resources Development (MOE), the Ministry of Commerce, Industry and Energy (MOCIE) and the Ministry of Labor (MOLAB) through the fostering project of the Lab of Excellency.

References

Fujioka, T., Aso, M. and Baba, J., 1995, "Comparison of Sliding and PID Control for Longitudinal Automated Platooning," *Society of Automotive Engineers*, SAE Paper No. 951898.

Hayashi, Y., 1998, "Expectations for Vehicle Control in the Next Generation," *Proceedings of the International Symposium on Advanced Vehicle Control*, pp. 1~8.

Holve, R., Protzel, P. and Naab, K., 1996, "Generating Fuzzy Rules for the Acceleration Control of an Adaptive Cruise Control System," *Proceedings of North American Fuzzy Information Processing*, pp. 451~455.

International Organization for Standardization 15622, 2002, *Transport Information and Control Systems — Adaptive Cruise Control Systems — Performance Requirements and Test Procedures*.

Jang, S., Kwon, S. J., Chun, J. H., Cho, K. Y. and Suh, M. W., 2005, "Development of the VR Simulation System for the Study of Driver's Perceptive Response," *Transactions of the Korea Society of Automotive Engineers*, Vol. 13, No. 2, pp. 149~156.

Kim, T. K., Park, Y. K. and Suh, M. W., 1999, "A Study on the Performance Characteristics of the VDC Vehicles," *Transactions of the Korea Society of Automotive Engineers*, Vol. 7, No. 9, pp. 146~157.

Korean Society of Automotive Engineers, 1996, *Automobile Technology Handbook*, Vol. 3, pp. 29~52.

Kubuzuka, T., 2002, "Perspective of ITS Technology: A Scenario," *Proceedings the International Symposium on Advanced Vehicle Control*, pp. 1~6.

Kwon, S. J., Fujioka, T., Omae, M., Cho, K. Y. and M. W. Suh., 2004, "A Study on the Model-Matching Control in the Longitudinal Autonomous Driving System," *International Journal of Automotive Technology*, Vol. 5, No. 2, pp. 134~144.

Lee, D. H. and Chang, K. S., 2000, "A Study on the Autonomous Cruise Control Using the Sliding Mode," *Transactions of the Korea Society of*

Automotive Engineers, Vol. 8, No. 2, pp. 92~101.

Lee, S. J., Hong, J. H. and Yi, K. S., 2001, "A Modeling and Control of Intelligent Cruise Control Systems," *Transactions of the Korea Society of Mechanical Engineers*, Vol. 25, No. 2, pp. 283~288.

Lee, S. W., 2003, "Intelligent Transport System in Japan," *Journal of the Korean Society of Automotive Engineers*, Vol. 25, No. 5, pp. 48~51.

Multigen Paradigm, 1999, *Multigen Creator User's Guide*.

Multigen Paradigm, 1999, *Vega Programmer's Guide*.

Redmill, K. A., Martin, J. I. and Özguner, Ü., 2000, "Virtual Environment Simulation for Image Processing Sensor Evaluation," *Proceedings of IEEE Intelligent Transportation Systems Conferences*, pp. 64~70.

Seto, Y., Murakami, T., Inoue, H. and Tange, S., 1998, "Development of a Headway Distance Control System," *Society of Automotive Engineers*, SAE Paper No. 980616.

Shladover, S. E., Desoer, C. A., Hedrick, J. K., Tomizuka, M., Walrand, J., Zhang, W. B., McMahon, D. H., Peng, H., Sheikholeslam, S. and McKeown, N., 1991, "Automatic Vehicle Control Developments in the PATH Program," *IEEE Transactions on Vehicular Technology*, Vol. 40, No. 1, pp. 114~130.

Suh, M. W., Kim, T. G., Yeo, J. W., Seok, C. S., Kim, Y. J. and Lee, J. C., 1999, "Development of Vehicle Model for Dynamic Analysis of ABS Vehicle," *Transactions of the Korea Society of Automotive Engineers*, Vol. 7, No. 2, pp. 228~241.

Suh, M. W., Koo, T. Y., Kwon, S. J., Shin, Y. S., Cho, K. Y. and Park, D. Y., 2002, "Development of the SVPG (Sungkyunkwan Univ. Virtual Proving Ground) : System Configuration and Application of the Virtual Proving Ground," *Transactions of the Korea Society of Automotive Engineers*, Vol. 10, No. 1, pp. 195~202.

Tamura, K. and Furukawa, Y., 1998, "Autonomous Vehicle Control System Equipped with a Navigation System," *Proceedings of the International Symposium on Advanced Vehicle Control*, pp. 361~367.

Wang, J. M. and Rajaman, R., 2002, "Adaptive Cruise Control System Design and Its Impact on Highway Traffic Flow," *Proceedings of the American Control Conference*, No. 5, pp. 3690~3695.

Won, M., Kim, S. S., Kang, B. B. and Jung, H. J., 2001, "Test Bed for Vehicle Longitudinal Control Using Chassis Dynamometer and Virtual Reality: An Application to Adaptive Cruise Control," *KSME International Journal*, Vol. 15, No. 9, pp. 1248~1256.